Exact two-dimensional plasma pair-correlation function in the Singwi-Tosi-Land-Sjolander approximation. II. Configuration-space analysis

P. Bakshi
Department of Physics and Center for Energy Research Boston College, Chestnut Hill, Massachusetts 02167

R. Calinon
Département de Physique, École Polytechnique Fédérale de Lausanne, CH-1007 Lausanne, Switzerland

K. I. Golden
Department of Electrical Engineering, Northeastern University, Boston, Massachusetts 02115

G. Kalman
Department of Physics and Center for Energy Research Boston College, Chestnut Hill, Massachusetts 02167

D. Merlini*
Department of Physics, College of William and Mary, Williamsburg, Virginia 23185
(Received 24 July 1978)

The configuration-space properties of the pair-correlation function in the Singwi, Tosi, Land, and Sjolander approximation scheme for a two-dimensional one-component plasma are derived here, using the exact solution in k space in the preceding paper. We also study in detail the effective static potential around a test particle for three cases representing weak, intermediate and strong coupling.

I. INTRODUCTION

The pair-correlation function for a strongly coupled one-component plasma has been the subject for study in a number of different approximation schemes.[1-5] However, until now, none of the approximation schemes has led to explicit analytical solutions, in either k or r space. The preceding paper[6] (hereafter referred to as I) provides an *exact* solution, for all strengths of the plasma parameter $\gamma = \beta e^2 = \kappa^2/2\pi n$, for the k-space correlation function $G(k)$ in the two-dimensional Singwi-Tosi-Land-Sjolander (STLS) approximation scheme. In the present paper, we analyze the properties and behavior of the corresponding configuration-space correlation function $g(r)$. While an exact analytical form for $g(r)$ for all γ is not obtainable, we have nevertheless: (i) developed the exact solution for certain γ values ($\gamma = 0$, $\gamma = 2$, and $\gamma \gg 1$) which represent reasonably well the weak-, intermediate-, and strong-coupling regimes (Sec. II); (ii) obtained complete short-range ($r \to 0$) analytical expressions for $g(r)$ for all γ (Sec. III); and (iii) developed an approach which provides the long-range ($r \to \infty$) behavior of $g(r)$ for all even-integral γ (Sec. IV). We have also obtained the $g(r)$ curves for various γ values (Sec. V) by means of a numerical Fourier transformation of the $G(k)$ results given in I.

These analytical and numerical results for $g(r)$ provide for the first time a model solution in which important physical properties such as the small-r or asymptotic (large-r) behavior of $g(r)$ can be studied uniformly for all γ, and for which questions such as the determination of the threshold for the onset of short-range order as a function of γ, and the limiting cases of weak ($\gamma \ll 1$), intermediate ($\gamma = 2$), and strong coupling ($\gamma \gg 1$), can be tackled effectively. We have also been able to study analytically the static effective potential around a test particle for those cases (Sec. VI). This model does not provide a liquid-solid phase transition (see Paper I); however, the inverse compressibility changes from positive to negative at $\gamma = 2$. This latter fact gives rise to a significant change in the behavior of the system, which will be well illustrated through the analysis of the effective potential.

II. EXACT SOLUTIONS FOR PARTICULAR γ VALUES

In Paper I, an implicit solution for the pair correlation in k space was obtained in the form [I, Eq. (10)]

$$\frac{G}{1+G}\left(\frac{\gamma}{2}+\frac{1}{1+G}\right)^{\gamma/2} = -\frac{1}{x^{\gamma+2}}\,, \tag{1}$$

$$\vec{x} = \vec{k}/\kappa,\quad \kappa^2 = 2\pi n\gamma,\quad \gamma = \beta e^2,\quad \beta^{-1} = k_B T\,.$$

For particular values of γ, the explicit form of $G(x)$ can be determined; a Fourier transform, followed by division by n, provides the configuration-space correlation function $g(r)$:

$$g(r)=\frac{1}{(2\pi)^2 n}\int d\vec{k}\, e^{i\vec{k}\cdot\vec{r}}G(\vec{k}) \tag{2a}$$

$$=\gamma\int_0^\infty dx\, xJ_0(\kappa r x)G(x). \tag{2b}$$

We now analyze $g(r)$ for three analytically tractable cases: $\gamma=0$, $\gamma=2$, and $\gamma\gg1$.

A. Debye limit $\gamma=0$

The Debye result is a limiting case of Eq. (1), obtained by setting $\gamma=0$:

$$G(x)=-1/(1+x^2). \tag{3}$$

Its Fourier transformation via Eq. (2) then provides

$$g(r)=-\gamma K_0(\kappa r), \tag{4}$$

the known Debye result,[7] which has the nonphysical small-r behavior

$$g(r)=\gamma\ln r+\cdots,\quad r\to0 \tag{5}$$

and the asymptotic form representing the Debye screening,

$$g(r)=-\gamma(\pi/2\kappa r)^{1/2}e^{-\kappa r}+\cdots,\quad r\to\infty. \tag{6}$$

B. Intermediate coupling $\gamma=2$

An explicit solution can also be constructed for $\gamma=2$, with Eq. (1) reducing to

$$G(x)=-1+x^2/(x^4+1)^{1/2}. \tag{7}$$

The Fourier transform, Eqs. (2), provides

$$g(r)=-(1/n)\delta(\vec{r})-[1/(2\pi)^2 n\kappa^2]\nabla^2 I(r), \tag{8}$$

with

$$I(r)=\int d\vec{k}e^{i\vec{k}\cdot\vec{r}}(1+x^4)^{-1/2}$$

$$=\kappa^2\int_0^\infty 2\pi x(1+x^4)^{-1/2}J_0(\kappa r x)dx$$

$$=2\pi\kappa^2 J_0(\kappa r/\sqrt{2})K_0(\kappa r/\sqrt{2}), \tag{9}$$

where the last step follows from a table of integrals.[8] Upon carrying out the Laplacian operation in Eq. (8), one obtains

$$g(r)=-\gamma J_1(\kappa r/\sqrt{2})K_1(\kappa r/\sqrt{2})$$

$$=-2J_1(\kappa r/\sqrt{2})K_1(\kappa r/\sqrt{2}). \tag{10}$$

This expression has the small-r expansion

$$g(r)=-1+\frac{3-4C}{16}(\kappa r)^2-\frac{(\kappa r)^2}{4}\ln\frac{\kappa r}{2\sqrt{2}}+O(\kappa^4 r^4), \tag{11}$$

where

$C=$ Euler's constant $=0.57721\ldots$.

Evidently, the probability $1+g(r)\to0$ as $r\to0$, and always remains positive, so that the small-r behavior is not in this sense anomalous. We shall return to this point in Sec. III, where the small-r behavior for arbitrary γ is discussed. An important feature of the correlation function (10) is that it clearly displays oscillations according to the properties of J_1, and specific exponential damping according to the properties of K_1. There is also a $1/r$ decay due to the combined J_1 and K_1 terms. For $\kappa r\gg1$, we have the asymptotic form

$$g(r)=-(2^{3/2}/\kappa r)e^{-\kappa r/\sqrt{2}}\cos(\kappa r/\sqrt{2}-\tfrac{3}{4}\pi)+\cdots. \tag{12}$$

We note that in contrast to the Debye limit ($\gamma=0$), the exponential decay is governed by $\kappa/\sqrt{2}$ rather than κ. Also, the algebraic decay follows r^{-1} rather than the $r^{-1/2}$ of Eq. (6). Since the damping and the oscillation have the same scale length $(\sqrt{2}/\kappa)$, one would not expect to see too many periods, a result borne out by the numerical results and the graphs for $g(r)$ given in Sec. V.

C. Strong coupling $\gamma\gg1$

For the analysis of strong coupling, it is convenient to rewrite Eq. (1) as

$$\frac{-G}{1+G}\left(1+\frac{2/\gamma}{1+G}\right)^{\gamma/2}=\frac{\frac{1}{2}\gamma}{\zeta^{\gamma+2}}, \tag{13}$$

where

$$\zeta=(\tfrac{1}{2}\gamma)^{1/2}x=\tfrac{1}{2}ka, \tag{14a}$$

and a is the "ion-circle radius,"

$$a=(\pi n)^{-1/2}. \tag{14b}$$

In the limit $\gamma\to\infty$, we obtain from Eq. (1)

$$\frac{-G}{1+G}\exp\left(\frac{1}{1+G}\right)=\frac{\frac{1}{2}\gamma}{\zeta^{\gamma+2}}, \tag{15}$$

which implies a step-function structure for G,

$$G=-1+\Theta(\zeta-1)=-1+\Theta(x-(2/\gamma)^{1/2}), \tag{16}$$

where

$$\Theta(y)=\begin{cases}1, & y>0\\ 0, & y<0.\end{cases}$$

The corresponding configuration-space correlation function is easily obtained from Eq. (2b) by noting the restricted range of integration implied by Eq. (16),

$$g(r)=-2\int_0^1 d\zeta\,\zeta J_0(2r\zeta/a)$$

$$=-\frac{a}{r}J_1(2r/a),\quad \gamma\to\infty. \tag{17}$$

This result, which seems to be indicative of long-range order, is valid for all r only when $\gamma \to \infty$. For any fixed γ, however large, one must probe further the structure of $G(k)$ during its transition from -1 to 0. As shown below, this transition occurs over a small, but significant, range of k, which modifies the large-r behavior of $g(r)$.

The analysis is facilitated if Eq. (2b) is transformed by an integration by parts to

$$g(r) = -\frac{\gamma}{\kappa r}\int_0^\infty dx\, x J_1(\kappa r x) G'(x). \tag{18}$$

This is an alternative expression for Eq. (2b), the Fourier transform in two-dimensional space, and, in fact, we will find this to be useful in other contexts as well (see Sec. VI). In this form, the $\gamma \to \infty$ limit for $g(r)$, Eq. (17) is recovered immediately by recognizing that

$$G'(x) = \delta(x - (2/\gamma)^{1/2}). \tag{19}$$

For any finite γ, however large, $G'(x)$ has a peak value of order $\gamma^{3/2}$ and a width of order $(1/\gamma)^{3/2}$ in the vicinity of $x = (2/\gamma)^{1/2}$, as can be seen from the expression [I, Eq. (8)]

$$xG'(x) = -G(1+G)[2+\gamma(1+G)] \equiv f(G). \tag{20}$$

The peak value of $f(G) \approx \frac{4}{27}\gamma$ is attained when $G \approx -\frac{1}{3}$. In terms of the scaled variable ζ of Eq. (14a), which is more appropriate for the strong-coupling regime (referring as it does only to the interparticle distance), we obtain

$$g(r) = -\frac{a}{r}\int_0^\infty d\zeta\, J_1((2r/a)\zeta) f(G), \tag{21}$$

$$\lim_{\gamma\to\infty} f(G) = \delta(\zeta - 1), \tag{22}$$

and, more generally,

$$\int_0^\infty f(\zeta)d\zeta = 1 + O\left(\frac{\ln\gamma}{\gamma}\right), \quad \gamma \gg 1. \tag{23}$$

Thus $f(G)$ plays the role of a "smeared δ function" near $\zeta = 1$, and its properties over a band $\Delta\zeta \sim O(1/\gamma)$ determine the precise structure of $g(r)$, according to Eq. (21). It should be noted that Eq. (21) is exact, and could be employed for analyzing the intermediate- or small-coupling regimes as well. For the strong-couplimg regime, it is clear that the structure of f plays no significant role as long as the scale length of oscillations of the Bessel function J_1 is much larger than the bandwidth of f, or $(r/a)\Delta\zeta \ll 1$, and the asymptotic result (17) remains valid for $r \ll \gamma a$. On the other hand, for $r \sim \gamma a$ and larger, the oscillations of J_1 within the band $\Delta\zeta$ reduce $g(r)$ significantly. Since $r \gg a$ for this regime, we can use the asymptotic form for J_1 and a change of variables, $\zeta = 1 + p/\gamma$, to obtain

$$g(r) \approx -(a/r)(a/\pi r)^{1/2}\,\mathrm{Re}\, e^{i2r/a} e^{-i3\pi/4}\bar{f}(r'),$$

$$\bar{f}(r') = \int_{-\gamma}^{\infty} dp\, e^{ipr'}\gamma^{-1} f(G)$$

$$\approx -\int_{-\infty}^{\infty} dp\, e^{ipr'} G(1+G)^2, \quad r' = 2r/a\gamma \tag{24}$$

where the relation between p and G is

$$p = \ln\gamma - \frac{1}{1+G} - \ln\left(-\frac{2G}{1+G}\right). \tag{25}$$

The integrand in the Fourier representation of $\bar{f}(r')$ has a width $\Delta p \sim O(1)$, centered around $p_0 \approx \ln\gamma - \frac{3}{2}$. Hence $\bar{f}(r')$ will decay on a scale $r' \sim O(1)$ or $r \approx a\gamma$ and have an oscillation characterized by $p_0 r'$ We have in Eq. (24) an example of a *scale transition*, as the behavior of $g(r)$ changes from a pure scale a for $r < \gamma a$ to the additional scale γa for $r \gtrsim \gamma a$. Physically, the "long-range order" indicated by Eq. (17) apparently cannot be maintained beyond the finite range $r \sim \gamma a$. It should be noted that

$$\bar{f}(r') = e^{ir'\ln\gamma} h(r'), \tag{26}$$

where $h(r')$ is independent of γ. Thus, apart from the phase shift, which varies as $\ln\gamma$, the entire effect for large γ is fully represented by some universal function of the scaled distance r', which can be numerically evaluated quite accurately.

III. SHORT-RANGE BEHAVIOR OF $g(r)$

The complete $g(r)$ for all r can be obtained explicitly only for particular values (or ranges) of γ, as was discussed in Sec. II. The short-range behavior, however, can be determined for arbitrary γ by taking a direct Fourier transform of the k-space solution.

There is an obvious interest in studying the small-r behavior of $g(r)$. In particular, the two-dimensional space, as it is known,[9] occupies a special position in this connection: if the correlation function is regarded as a function of the (continuously varying) dimensionality parameter ν, where $3 > \nu > 1$, then according to the exact theory, $1 + g^{(\nu)}(r)$, approaches zero in a nonanalytic fashion, with an essential singularity $\exp(-a/r^{\nu-2})$ as $r \to 0$ for all $\nu > 2$; on the other hand, for $\nu < 2$, $1 + g^{(\nu)}(r)$ approaches a nonzero limit $[0 < 1 + g^{(\nu)}(0) < 1]$, and for $r \to 0$ goes as $1 + g^{(\nu)}(0) + br^{2-\nu}$. In the two-dimensional case, however, $1 + g^{(2)}(r) \to cr^{\gamma}$, and thus the analytic character manifestly changes with the coupling strength γ, which is certainly not the case in other dimensions.

It has also been shown recently,[10] through a configuration-space formulation of the basic equations, that various known approximation schemes, including the present one, are plagued by problems of nonphysical behavior in the small-r domain. It will

be rather instructive to see how, and to what extent, the requirements of the exact theory and the problems of nonphysical behavior combine into the precise analytic form we can display for this scheme.

A. Derivation of results

The small-r behavior of $g(r)$ is related to the large-k behavior of $G(k)$, and the structure of the small-r series for $g(r)$ can be systematically inferred from Eq. (2b). For all values of $\gamma \neq 0$,

$$g(r=0) = \gamma \int_0^\infty dx\, xG(x) = -1\,, \tag{27}$$

a relation most easily obtained from [I, Eq. (6)]

$$u(x) = \gamma \int_0^x dz\, zG(z) \tag{28}$$

and [I, Eq. (3)]

$$G(x) = -\frac{1+u(x)}{x^2+1+u(x)} \tag{29}$$

by noting that according to Eq. (1), $G(x\to\infty)\to 0$ as $x^{-2-\gamma}$, which requires $g(0) \equiv u(x\to\infty)$ to be -1. Physically, Eq. (27) reflects the fact that the probability $\sim[1+g(r)]$ of finding two particles with zero separation ($r\to 0$) must vanish. To determine its precise dependence on the separation distance, we evaluate the next term in $g(r)$ by subtracting Eq. (27) from Eq. (2b):

$$1+g(r) = \gamma \int_0^\infty dx\, x[J_0(\kappa r x) - 1]G(x)\,. \tag{30}$$

The subsequent analysis and the results differ, depending on whether $\gamma > 2$, $\gamma = 2$, or $\gamma < 2$.

For $\gamma > 2$, the next term is of order $\kappa^2 r^2$, with its coefficient given by the convergent integral

$$a_2 = \tfrac{1}{4}\gamma \int_0^\infty dx\, x^3 G(x)\,. \tag{31}$$

This is proportional to the second moment of $G(x)$ over $\vec{x}$ space, and is most easily evaluated by using Eq. (29) in the form

$$\int_0^\infty dx\, x^3 G(x) + \int_0^\infty dx\, xG(x)(1+u) = \tfrac{1}{2}\int_0^\infty dx\, x^2 u'(x) \tag{32}$$

and the differential form of Eq. (28), $du = \gamma x G(x) dx$. The result is

$$a_2 = 1/4(\gamma - 2)\,. \tag{33}$$

For $\gamma = 2$, the integral in Eq. (31) diverges, indicating a stronger-than-r^2 behavior for Eq. (30). By defining $x^4 G(x) = D(x)$, $D(x\to\infty) = -\frac{1}{2}$, and scaling $x \to x/\kappa r$, we obtain

$$1+g(r) = 2\kappa^2 r^2 \int_0^\infty \frac{dx}{x^3}[J_0(x) - 1]D(x/\kappa r) \to -\tfrac{1}{4}\kappa^2 r^2 \ln \kappa r + b_2 \kappa^2 r^2\,, \quad \gamma = 2 \tag{34}$$

in agreement with Eq. (11), as can be shown by dividing the range of integration in Eq. (34) into various domains and using appropriate limiting forms for J_0 and D.

For $\gamma < 2$, the leading term is r^γ, as can be seen by rewriting Eq. (30) as

$$\begin{aligned} 1+g(r) &= -\gamma \int_0^r dr'\, \kappa \int_0^\infty dx\, x^2 J_1(\kappa r' x) G(x) \\ &= -\gamma \int_0^r dr'\, \kappa^\gamma r'^{\gamma-1} \int_0^\infty \frac{dx}{x^\gamma} J_1(x)\bar{D}(x/\kappa r')\,, \end{aligned} \tag{35}$$

with $\bar{D}(x) = x^{2+\gamma}\bar{G}(x)$, $\bar{D}(x\to\infty) = -(1+\frac{1}{2}\gamma)^{-\gamma/2}$. The last integral remains convergent even when we let $r' \to 0$ in the argument of $\bar{D}$. Then, to leading order,

$$\begin{aligned} &1+g(r) = C_\gamma (\kappa r)^\gamma\,, \quad \gamma < 2 \\ &C_\gamma = \frac{\Gamma(1-\frac{1}{2}\gamma)}{\Gamma(1+\frac{1}{2}\gamma)} \quad \frac{1}{2^\gamma (1+\frac{1}{2}\gamma)^{\gamma/2}}\,. \end{aligned} \tag{36}$$

The leading terms for the various cases can now be summarized as

$$g(r) = -1 + \begin{cases} a_2 \kappa^2 r^2\,, & \gamma > 2 \quad (37a) \\ -\tfrac{1}{4}\kappa^2 r^2 \ln \kappa r + b_2 \kappa^2 r^2\,, & \gamma = 2 \quad (37b) \\ C_\gamma \kappa^\gamma r^\gamma\,, & \gamma < 2\,. \quad (37c) \end{cases}$$

By continued subtractions and use of the asymptotic properties of $G(x)$, one can develop higher-order terms. For any $\gamma = 2m + \alpha$, $m = 0, 1, \ldots$; $0 < \alpha < 2$, the first nonanalytic term is r^γ, preceded by a series in powers of r^2 up to r^{2m}, the coefficients being the corresponding moments of $G(x)$, which can be evaluated explicitly. The appearance of $r^{2m}\ln r$ terms is a common feature for all even γ. The results of Eqs. (37) are in agreement with the small-r analysis based on a configuration-space formulation[10] of the basic equations of this model; the advantage here lies in the explicit determination of C_γ, Eq. (36).

B. Discussion of results

We note the following properties of the small-r results in Eqs. (37).

(i) The small-r limit of the Debye result, Eq. (4), is contained in Eq. (37c), which reduces precisely to $\gamma(\ln\frac{1}{2}\kappa r + C)$ to order γ when we expand C_γ, and $(\kappa r)^\gamma \approx 1 + \gamma \ln \kappa r$. The nonphysical [$g(r\to 0) \to -\infty$] behavior of the Debye result can thus be seen to be due to restricting the expansion to order γ; keeping higher-order terms in γ would remove

the anomalous small-r behavior of the Debye result.

(ii) For $\gamma=2$, Eq. (37b) agrees with the small-r expression of the exact solution, Eq. (11).

(iii) Equation (37a) and subsequent terms in the analytic series in powers of r^2 agree with the small-r expansion of Eq. (17) describing the domain $\gamma \gg 1$ provided only the leading terms in γ are retained in the former. The occurrence of inverse powers of γ generates the required change of scale (by means of the relation $\kappa^2/\gamma = 2\pi n = 2/a^2$) from the Debye length κ^{-1}, appropriate for small and moderate γ's, to the interparticle distance $(\pi n)^{-1/2} = a$, appropriate for large γ.

(iv) The slope $g'(0)$ is infinite for $\gamma < 1$, $(\frac{2}{3})^{1/2}$ for $\gamma = 1$, and zero for $\gamma > 1$.

(v) Equation (37) also shows that the relative probability $1+g(r)$ has the physically required positive character for all γ in the present approximation scheme; this is in contrast to results obtained for other schemes.[10]

(vi) Physically, one would also require $1+g(r) \sim \exp[-\beta\phi(r)] \sim r^\gamma$ as $r \to 0$ for any γ, where $\phi(r)$ is the bare (Coulomb) potential; this is indeed so for $\gamma < 2$ in this scheme, but for $\gamma \geq 2$, an anomalous r^2 ($r^2 \ln r$ for $\gamma = 2$) behavior sets in, which dominates over the physically expected r^γ. This situation is nevertheless an improvement over the three-dimensional case for the Singwi-Tosi-Land-Sjolander (STLS) scheme, which violates[10] the corresponding physical requirement for all γ.

(vii) The special values $\gamma = 2m$ introduce the $r^{2m} \ln r$ behavior, which *appears* to be qualitatively different from the pure power-law results for $\gamma \neq 2m$. It can be shown, however, that $g(r,\gamma)$ is a smooth function of γ at $\gamma = 2m$, and, in fact, the coefficient of r^{2m} (including the $\ln r$ term) for $\gamma = 2m$ is precisely the nonvanishing difference between the nonanalytic r^γ and the analytic r^{2m} terms as $\gamma \to 2m$.

IV. LONG-RANGE BEHAVIOR OF $g(r)$

The long-range behavior of $g(r)$ is governed by the singularity structure of $G(k)$ in the complex k plane. From Eqs. (1) and (14a),

$$x = (\tfrac{1}{2}\gamma)^{-\gamma/2(\gamma+2)}(-1)^{1/(\gamma+2)}$$

or

$$\zeta = (\tfrac{1}{2}\gamma)^{1/(\gamma+2)}(-1)^{1/(\gamma+2)} \tag{38}$$

are the singularities of $G(k)$. For $\gamma = 0$, one recovers $x = \pm i$ as simple poles, which is expected from the Debye solution, Eq. (3). It is clear, by inspection, that this will provide the correct exponential behavior $e^{-\kappa r}$. A detailed contour integration leads to the additional decay $r^{-1/2}$. For $\gamma = 2$, there are four branch cuts at $x = \zeta = \pm e^{\pm i\pi/4}$. Again, it is clear that this will give a damped oscillation $\exp[-(\kappa r/\sqrt{2})(1 \pm i)]$. To obtain the complete large-r behavior, consider Eq. (2b) in the alternative form

$$g(r) = \tfrac{1}{2}(I^{(1)} + I^{(2)}),$$
$$I^{(1),(2)} = \gamma \int_0^\infty dx\, x H_0^{(1),(2)}(\kappa r x) G(x). \tag{39}$$

$I^{(1)}$ is then evaluated by closing the contour around the first quadrant on the large circle $|x| \to \infty$ where $x = |x| e^{i\theta}$ and $0 \leq \theta \leq \frac{1}{2}\pi$, and coming down along the positive imaginary axis. The branch cut is drawn at the angle $\frac{1}{4}\pi$ from $e^{i\pi/4}$ to infinity. $I^{(2)}$ is evaluated by a similar construction in the fourth quadrant. It can be shown (see the Appendix) that, owing to the properties of the Hankel functions $H_0^{(1)}$ and $H_0^{(2)}$, the two contributions along the imaginary axis compensate exactly for any function with the symmetry $G(x) = G(-x)$. Hence only the two branch-cut contributions survive, and a detailed calculation gives the correct large-r behavior, Eq. (12).

A similar procedure applies immediately to all even $\gamma = 2m$, since the symmetry condition $G(x) = G(-x)$ is satisfied, and provides the result, based on the singularities nearest to the real axis,

$$g(r) \approx \mathrm{Re}(2a/r)(\zeta_0/\sqrt{\gamma}) e^{i(2r/a)\zeta_0}, \quad r \gg a. \tag{40}$$

In obtaining this result, we have used from Eq. (38) the fact that the singularities in the ζ plane, ζ_l, for a given γ all lie on a circle,

$$|\zeta_l| = (\tfrac{1}{2}\gamma)^{1/(\gamma+2)} = 1 + \frac{1}{\gamma+2}\ln(\tfrac{1}{2}\gamma) + \frac{1}{2}\left(\frac{1}{\gamma+2}\right)^2 (\ln\tfrac{1}{2}\gamma)^2 + \cdots, \tag{41}$$

and have phase factors

$$e^{i\pi(2l+1)/(\gamma+2)}, \quad l = 0, 1, \ldots, \gamma+1. \tag{42}$$

It can also be shown from Eq. (20), which reduces to $xG' = -\gamma G^3$ when $|G| \to \infty$, that each singularity is a square-root-type branch cut. The two singularities nearest to the real axis, with phase factors $e^{\pm i\pi/(\gamma+2)}$, make the most significant contributions.

For $\gamma \gg 1$, $|\zeta| \to 1$, and the most significant singularities occur at

$$\zeta \approx 1 + (\gamma+2)^{-1}\ln(\tfrac{1}{2}\gamma) \pm i\pi/(\gamma+2) \approx 1 + (1/\gamma)\ln(\tfrac{1}{2}\gamma) \pm i\pi/\gamma, \tag{43}$$

which provide a contribution proportional to $e^{i\zeta 2r/a} \approx e^{i2r/a} e^{-2\pi r/\gamma a}$. The power-law decay arises by integration around the entire branch cut. These results, Eqs. (40)–(43), are in agreement with Eq. (24), and in fact specify the precise nature and scale size for the decay of $\bar{f}(r')$ for $r > \gamma a$. Accord-

ing to Eqs. (41) and (42), there are further singularities, $l=1,\ldots,$ which provide the same oscillation but faster exponential decays when $r>\gamma a/l$. The oscillation scale length does not vary much with γ, since $\mathrm{Re}\zeta_0=|\zeta_0|\cos[\pi/(\gamma+2)]$ only ranges between 0.95 and 1.1 for $\gamma=4$ to ∞. The maximum ≈ 1.1 is reached around $\gamma=10$; thus the "tightest packing" in terms of the probability variations indicated by $g(r)$ occurs for the intermediate coupling $\gamma\approx 10$! The numerical results of the next section confirm this prediction. While we have not discussed the complex-variable analysis for $\gamma \neq 2m$, the physical results can be expected to be continuous in γ, and thus the methods here are sufficient to understand the nature of $g(r)$ for any γ.

V. NUMERICAL RESULTS

The correlation function $g(r)$ can be computed by using Eq. (2b) and the numerically obtained $G(x)$ from I, Eq. (10). The oscillatory nature of $J_0(\kappa r x)$ with known zeros allows integration between the zeros by a Lobatto quadrature. Our numerical results for $\gamma=1$, 1.5, 2, and 2.5 are displayed in Fig. 1 and those for $\gamma=3$, 5, 10, and 30 in Fig. 2.

Various analytical results in Secs. II–IV are fully confirmed by these figures and other numerical results not presented here in detail. In particular: (i) the slope $g'(0)$ varies from ∞ for $\gamma<1$, to $(\frac{2}{3})^{1/2}$ for $\gamma=1$, to 0 for $\gamma>1$; (ii) oscillation becomes more prominent for increasing γ; (iii) wavelength

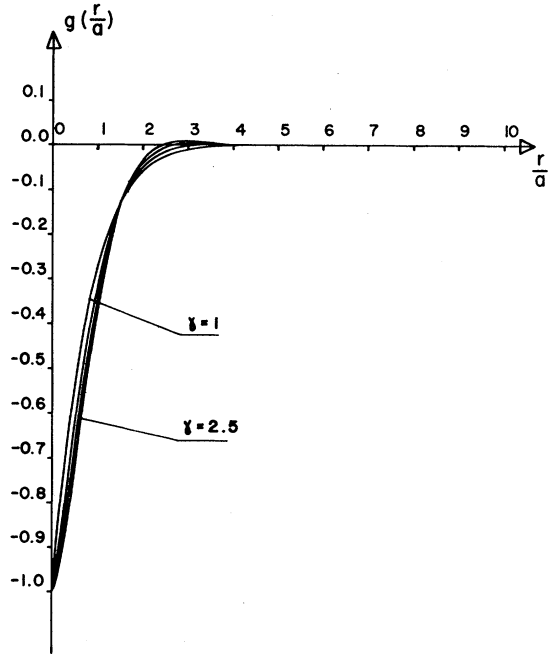

FIG. 1. Pair-correlation function $g(r/a)$ for $\gamma=1$, 1.5, 2, and 2.5.

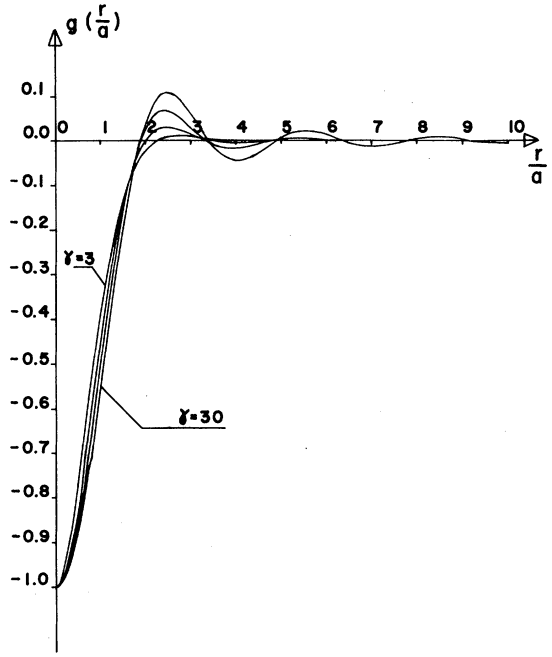

FIG. 2. Pair-correlation function $g(r/a)$ for $\gamma=3$, 5, 10, and 30.

is shortest around $\gamma\approx 10$; (iv) pure $r^{-1}J_1(2r/a)$ behavior, Eq. (17), is achieved to a good approximation by $\gamma=30$; and (v) in general, the fluidlike state with intermediate-range order is quite evident in Fig. 2 with the larger γ values. Our computations were not carried out far enough in r for large γ to assess the decay rates for $r>\gamma a$ numerically.

VI. EFFECTIVE POTENTIAL

Although our main interest in this paper has been the analysis of the pair-correlation function, additional information can be obtained from a related object, the effective static potential surrounding a fixed test particle (impurity) in the system. This effective potential $\Phi(r)$, which is obviously distinct from the bare Coulomb potential $\phi(r)=-e^2\ln r$ owing to many-body effects, should also be distinguished from the potential of the average force $\Psi(r)$, defined by $g(r)=e^{-\beta\Psi(r)}-1$. $\Phi(r)$ is determined through linear-response theory with the aid of the static dielectric response function $\epsilon(k)$. As such, it represents a good approximation to the actual potential around a test particle insofar as the linear approximation is valid. Moreover, the source of $\Phi(r)$ is *not* in equilibrium with the system, while that of $\Psi(r)$ is. These difference explain the different characters of $\Phi(r)$ and $\Psi(r)$, as borne out by the subsequent calculations.

Our interest in $\Phi(r)$ also stems from the obser-

vation put forward in Paper I, that $\int \Phi(r) d\vec{r}$ changes from positive to negative as γ exceeds 2. While for small distances both $\Phi(r)$ and $\phi(r)$ are postive, this phenomenon indicates the emergence of significant negative domains in $\Phi(r)$ for larger distances. This will become evident from the detailed results in this section.

The effective potential is given by

$$\Phi(x) = \phi(x)/\epsilon(x), \quad \phi(x) = 2\pi e^2/k^2 = 1/n\beta x^2, \tag{44}$$

and according to I, Eqs. (13)–(15),

$$\beta n\Phi(x) = (1/x^2)\{1 - [1 + G(x)]/x^2\}. \tag{45}$$

Taking a Fourier transform provides the dimensionless effective potential[11]

$$\beta\Phi(r) = \gamma \int_0^\infty dx\, x J_0(\kappa r x)\beta n\Phi(x). \tag{46}$$

As in the case of the pair-correlation function, we can obtain explicit solutions for the special cases $\gamma \to 0$, $\gamma = 2$, and $\gamma \gg 1$. For the Debye case ($\gamma = 0$) substitution of Eq. (3) into Eq. (45) provides the screened effective potential

$$\beta\Phi(r) = -g(r) = \gamma K_0(\kappa r). \tag{47}$$

The effective potential for small r is identical to the bare potential,[11]

$$\beta\Phi(r) \to -\gamma \ln \kappa r, \quad r \to 0 \tag{48}$$

while it becomes exponentially damped for large r:

$$\beta\Phi(r) \to \gamma(\pi/2\kappa r)^{1/2} e^{-\kappa r} + \cdots, \quad r \to \infty. \tag{49}$$

Although for large r the effective potential deviates substantially from the bare potential, it always remains positive definite, as expected on physical grounds. We also note that if $\beta\Psi(r) \ll 1$, then $-\beta\Psi(r) \approx g(r) = -\beta\Phi(r)$; $\Phi(r) = \Psi(r)$ is the distinguishing feature of the Debye approximation.

For $\gamma = 2$, it is convenient to use the alternative representation, analogous to Eq. (18), obtained by an integration by parts of Eq. (46),

$$\beta\Phi(r) = -\frac{\gamma}{\kappa r} \int_0^\infty dx\, x J_1(\kappa x r)\beta n\Phi'(x). \tag{50}$$

Differentiating Eq. (45) and using Eq. (7), we find

$$\beta n\Phi'(x) = -(2/x)\beta n\Phi(x) + G'(x), \tag{51}$$

which, by virtue of Eqs. (18) and (50), leads to

$$\beta\Phi(r) = \chi(r) + g(r), \tag{52}$$

with

$$\chi(r) = \frac{2\gamma}{\kappa r} \int_0^\infty dx J_1(\kappa r x)\beta n\Phi(x). \tag{53}$$

Then

$$\frac{d}{dr}(r^2\chi) = \frac{2\gamma}{\kappa} \int_0^\infty dx\, \frac{d}{dr}[r J_1(\kappa x r)]\beta n\Phi(x)$$
$$= 2\gamma r \int_0^\infty dx\, x J_0(\kappa x r)\beta n\Phi(x)$$
$$= 2r\beta\Phi(r), \tag{54}$$

or

$$\chi(r) + \tfrac{1}{2} r\chi'(r) = \beta\Phi(r). \tag{55}$$

Comparing Eqs. (52) and (55), we find

$$g(r) = \tfrac{1}{2} r\chi'(r), \tag{56}$$

and Eq. (52) reduces to

$$\beta\Phi(r) = g(r) - \int_r^\infty \frac{2g(r')}{r'} dr', \tag{57}$$

with $g(r)$ given explicitly by Eq. (10). For small r, since $g(r) \to -1$, the integral in (57) dominates and again we appropriately recover the bare potential[11]

$$\beta\Phi(r) = -2\ln r = -\gamma \ln r, \quad r \to 0. \tag{58}$$

For large r, the integral is an order of $1/r$ smaller than $g(r)$, so that one obtains

$$\beta\Phi(r) \approx g(r) \approx -(2^{3/2}/\kappa r)e^{-\kappa r/\sqrt{2}} \times \cos(\kappa r/\sqrt{2} - \tfrac{3}{4}\pi), \quad \kappa r \gg 1. \tag{59}$$

We note that the potential now has developed an oscillating tail with oscillations apparently strong enough for $\int \Phi(r) d\vec{r} = 0$ as required by I, Eq. (16). We also note that $\Phi(r) \approx -\Psi(r)$ for large r.

For the regime $\gamma \gg 1$, one can invoke the step-function character of $G(x)$, as in Eq. (16), to obtain, using Eq. (46) and the scaling equation (14a),

$$\beta\Phi(r) = \gamma \int_0^1 \frac{d\zeta}{\zeta}(1 - f) J_0(2r\zeta/a) + \gamma \int_1^\infty \frac{d\zeta}{\zeta} J_0(2r\zeta/a) - \tfrac{1}{2}\gamma^2 \int_1^\infty \frac{d\zeta}{\zeta^3} J_0(2r\zeta/a), \tag{60}$$

where, by virtue of I, Eq. (11),

$$f = (1 + G)/x^2 = 1 + \zeta^2(1 - 2/\gamma) + \cdots. \tag{61}$$

The last term in Eq. (60), of order γ^2, represents the leading contribution for large γ, over a wide range of r,

$$\beta\Phi(r) \approx -\tfrac{1}{2}\gamma^2 \int_1^\infty \frac{d\zeta}{\zeta^3} J_0(2r\zeta/a) \tag{62a}$$
$$= \tfrac{1}{4}\gamma^2 (a/r)[J_1(2r/a) + O(a^2/r^2)], \quad r \gg a$$
$$\approx -\tfrac{1}{4}\gamma^2 g(r). \tag{62b}$$

For $r > \gamma a$, the exponential damping of the type discussed in Sec. II C will apply to the screened effective potential as well, and Eq. (62b) remains valid to leading order in γ, even though (62a) is

not. For $r \sim a$, (62a) must be used rather than (62b), and a more explicit form is

$$\beta\Phi(r) \approx -\frac{\gamma^2}{4}\left[J_0(2r/a) - \frac{r}{a}J_1(2r/a) + \frac{2r^2}{a^2}\left(C + \ln\frac{r}{a} + \sum_{k=1}^{\infty}\frac{(-1)^k(r/a)^{2k}}{2k(k!)^2}\right)\right]. \tag{63}$$

For small r, Eq. (63) leads to the limit $-\frac{1}{4}\gamma^2$. However, the second term of order γ in Eq. (60) develops a $\ln r$ behavior as $r \to 0$, which dominates over the large but fixed $-\frac{1}{4}\gamma^2$. The first term of order γ remains bounded as $r \to 0$, and is less important than the other terms, so that

$$\beta\Phi(r) \approx -\gamma \ln(2r/a) - \tfrac{1}{4}\gamma^2 + O(\gamma). \tag{64}$$

The potential now changes sign for small enough r to ensure that $\int \Phi(r)d\vec{r} < 0$. Thus a test particle is surrounded primarily by regions in which particles of like charge experience an *attractive* rather than a *repulsive* force.

From these results we observe that in the three cases $\gamma \ll 1$, $\gamma = 2$, and $\gamma \gg 1$ the small-r behavior is given by

$$\beta\Phi(r) = -\gamma \ln r, \quad r \to 0 \tag{65}$$

which is just the bare potential,[11] as is to be expected on physical grounds. It can be shown that this result indeed holds for arbitrary γ.

For large r, we observe that $\beta\Phi(r)$ becomes proportional to $g(r)$ in the three cases $\gamma \ll 1$, $\gamma = 2$, and $\gamma \gg 1$, but the proportionality constant varies with γ. This could also be inferred directly from the definition of $\Phi(x)$, Eq. (45), which can be rewritten

$$-x^4 \beta n \Phi(x) = 1 - x^2 + G(x). \tag{66}$$

A Fourier transform then provides

$$-\nabla^4(\beta\Phi(r)) = g(r), \quad r \neq 0 \tag{67}$$

where we have omitted the δ-function and its derivative terms. It is easily verified that Eq. (67) correctly predicts the detailed relationship given for the three cases $\gamma = 0$, $\gamma = 2$, and $\gamma \gg 1$ in Eqs. (47), (59), and (62b). In fact, Eq. (67) is valid for all γ (for $r \neq 0$), and can be used directly to determine $g(r)$ if $\Phi(r)$ is known. With proper accounting of the source terms, it can also be used to solve for $\Phi(r)$ when $g(r)$ is given. Finally, the difference between $\Phi(r)$ and $\Psi(r)$ becomes evident from Eq. (67).

VII. CONCLUSIONS

In this and the preceding paper, we have completed the study of the properties and implications of a closed-form analytic solution of the pair-correlation function obtained for the two-dimensional ocp for arbitrary coupling strength in the STLS approximation. While Paper I was devoted to the exposition of the method of obtaining the solution in k space and to the study of results derivable from it directly without obtaining the configuration-space representation of the pair-correlation function, in this paper we have analyzed the latter, $g(r)$, along with $\Phi(r)$, the effective potential surrounding an impurity in the system. We have been able to obtain explicit results over the entire r domain for the three cases $\gamma \ll 1$, $\gamma = 2$, and $\gamma \gg 1$, representing the weak-, intermediate-, and strong-coupling regimes. In addition, we have also obtained the short-range ($r \to 0$) behavior of $g(r)$ for all γ and the long-range ($r \to \infty$) behavior of $g(r)$ for all even integral γ. Numerically calculated $g(r)$ curves have also been presented for the full range of coupling strengths.

We can assess here the relevance of these results in the broader context of what is known to date for other approximation schemes in three- as well as two-dimensional ocp's. As pointed out in the Introduction, (and in Paper I), the STLS scheme in two dimensions is unique in that it provides a closed-form solution for $G(k)$. This in turn allows us to obtain a number of explicit results for $g(r)$, as listed above. The most noteworthy features that emerge from this study are as follows.

(i) Exact solutions for intermediate ($\gamma = 2$) and strong ($\gamma \gg 1$) coupling are developed which provide for the first time, in any scheme, in any dimensions, explicit analytical results for $g(r)$ in those regimes.

(ii) The existence of a "liquid" state, characterized by an *intermediate-range order* is the most remarkable feature of this model. This "liquid" state emerges gradually with increasing γ without any sharp phase transition. The representation [Eq. (17)] of $g(r)$ for $\gamma \gg 1$ indicative of this intermediate-range order remains valid over a wide range of r, $r \ll \gamma a$; $g(r)$ displays oscillations within this range with a wavelength πa and an algebraic decay $\sim (r/a)^{-3/2}$, both independent of γ. For $r \gtrsim \gamma a$ a scale transition occurs, and an exponential decay $e^{-2\pi r/\gamma a}$ becomes significant, which eventually becomes dominant for $r \gg \gamma a$. In this sense we can only talk about an *intermediate-* and not a *long-range* order. This is of course in agreement with the feature already noted in Paper I that $G(k)$ does *not* have a singularity on the real axis, and thus no liquid-solid phase transition is allowed by this model.

While there are *no* other analytical results available, either in two or three dimensions, one can compare our results with the Monte Carlo results[12] in three dimensions to see if any common features

prevail. Indeed, the latter results also indicate a clear emergence of a "liquid" state for $\Gamma \gg 1$ ($\Gamma = \beta e^2/a$, where a is the ion-sphere radius),[12] with a periodic variation in $g(r)$ with wavelength $\approx \frac{3}{2} a$. The successive peaks in $g(r)$ decline with increasing r; the precise functional form, however, cannot be inferred from the limited data. The periodicity and a series of peaks with monotonically decreasing amplitude are common features in two and three dimensions. A difference between the two cases is the Γ dependence of the height of the first and successive peaks in three dimension, in contrast to the γ independence of the two-dimensional result, Eq. (17). Even though the height of the first peak of $g(r)$ (Fig. 2) continues to increase up to $\gamma = 30$, the asymptotic ($\gamma \gg 1$) result, Eq. (17), does not differ much from the $\gamma = 30$ curve for $g(r)$, and the γ-independent regime is essentially attained for $\gamma \gtrsim 50$. This is in contrast to the three-dimensional (Monte Carlo) results, where the height of the first peak of $g(r)$ continues to increase right up to the phase transition around $\Gamma \approx 155$. It should be noted that the γ independence in the two-dimensional STLS model is the direct consequence of the step-function character of $G(k)$ or, equivalently, the δ-function character of $G'(k)$. The three-dimensional Monte Carlo $G(k)$ does not have this character, and attains increasingly larger positive values for its first peak as Γ is increased. It can be easily shown that a Γ-independent asymptotic liquid state would result in three dimensions as well if $G(k)$ had the step-function character. A related, interesting question then is whether or not other two-dimensional schemes lead to a γ-independent asymptotic state; preliminary results[13] for the more sophisticated Totsuji-Ichimaru scheme indicate that some γ dependence will prevail even for large γ, thus pointing to a possible defect in the STLS two-dimensional model.

(iii) A related point to be noted is the difference in the singularity structure in the complex k plane of $G(k)$ in the model studied and in three dimensions. The three-dimensional $G(k)$ develops complex poles[14] for $\Gamma > 0$ which approach the real axis with increasing Γ, heralding the phase transition which sets in at $\Gamma \approx 155$ when one of the poles reaches the real axis. The pole in the vicinity of the real axis for $155 > \Gamma \gg 1$ results in the $G(k)$ with the characteristic pronounced positive peak. On the other hand, the singularities of the two-dimensional $G(k)$ in the STLS scheme are of the branch-cut type, which, even though they approach (although never reach) the real axis as γ increases, are damped by a $1/\sqrt{\gamma}$ factor, ensuring that on the real axis $G(k) \sim [k_0/\gamma(k - k_0)]^{1/2}$ remains bounded and small; $G'(k)$, however, does develop a peak and a behavior resembling that of $G(k)$ in three dimensions; hence the different behavior already noted.

(iv) The study of the short-range behavior of $g(r)$, in Sec. III, shows explicitly the γ dependence of the approach to zero for $1 + g(r)$ as $r \to 0$. The appearance of an anomalous r^2 term overwhelming the requisite r^γ behavior for $\gamma > 2$ is a characteristic feature of the present approximation. While this result has been obtained elsewhere,[10] the present method offers the advantage of providing an explicit coefficient for the r^γ term in Eq. (37), and allows one to see how the Debye result, with its nonphysical small-r behavior, is the direct consequence of an improper expansion of r^γ to order γ. It also explains the occurrence of terms like $r^{2m} \ln r$ for even integral γ to be the result of the confluence of the analytic (r^{2m}) and the non-analytic (r^γ) parts of the full solution. One can also infer, from our method of derivation here, that the short-range anomaly would be avoided only if the first few moments of $G(k)$, i.e., $\int k^{2m} G(k) d\vec{k}$, vanish identically when $\gamma = 2m + \alpha$, where $m = 0, 1, 2, \ldots$ and $0 < \alpha < 2$.

As pointed out elsewhere,[10] the short-range anomaly is a common problem for many approximation schemes in both two and three dimensions; it is a feature of the two-dimensional schemes that the anomaly is γ dependent, occurring only for $\gamma \geq 2$, in contrast to the three-dimensional situation (in STLS, as well as other schemes) where the anomaly occurs for all Γ's.

(v) The long-range behavior of $g(r)$, described in Secs. II and IV, also shows clear variations with γ. The damping is exponential in the cases studied explicitly, and the scale length in the strong-coupling regime can be traced to the singularity structure of $G(k)$ in the complex k plane. It is a remarkable feature of the STLS model (in two dimensions) that this singularity structure can be seen explicity, even for intermediate- and strong-coupling regimes, in contrast to other studies (mostly in three dimensions) which can assess the singularity structure only by perturbative methods.

Besides the overall damping, one finds the oscillatory behavior already noted, which for $\gamma \geq 4$ exhibits only a slight variation of wavelength with γ. For $\gamma \gg 1$, the wavelength approaches the asymptotic limit πa. The detailed analysis in Sec. IV, where the order $1/\gamma$ corrections to the wavelength and the corresponding damping rate are given explicitly, shows that several of the singularities near the real axis, having the same oscillation but different damping rates, will combine to produce the asymptotic "liquid" state for $g(r)$, and the gradual departure of $g(r)$ from that state as $1/\gamma$ increases can be understood in this sense.

(vi) While, as we have noted on several occa-

sions, there is no phase transition generated by the model we have studied, the other well-established feature of the three-dimensional ocp, namely, that the inverse isothermal compressibility becomes 0 and then negative for moderate values of Γ, is shared by the two-dimensional STLS model, which exhibits this feature at $\gamma = 2$. The physical quantity that is most sensitive to this change of physical state is the effective potential $\Phi(r)$ around an impurity which we have studied in addition to $g(r)$ for the quoted γ domains. From the detailed study and from the moment condition $\int \Phi(r)d\vec{r} \gtrless 0$ for $\gamma \lesseqgtr 2$, we could infer that the general behavior of $\Phi(r)$ is such that, while for $\gamma = 0$ it represents pure exponential screening, it develops together with $g(r)$ small asymptotic oscillations which become more dominant as γ increases, to the extent that $\int \Phi(r)d\vec{r}$ changes sign [while, of course, $\int g(r)d\vec{r} = -1$, independently of γ]. The physical implication of this effect, that is, the predominance of attraction between like charges as mediated by the medium, is a remarkable strong-coupling phenomenon, whose analytic details are exhibited here for the first time.

In these two papers we have provided an exact analysis of a simple but reasonable model for strongly coupled plasmas. The main lessons to be learned from exact solutions are *insights* which can be applied to related problems which cannot be solved exactly. In this light, the analysis here will have an obvious bearing on understanding the widely studied three-dimensional STLS model, the Totsuji-Ichimaru schemes in two and three dimensions, and possibly some other schemes as well. The analytical forms obtained here, and methods developed here, may serve as starting points for approximation schemes in the study of those models. Developing a sense for the structure of $G(k)$ or $g(r)$ over the full range of γ values is the major accomplishment here, and is lacking in other schemes.

ACKNOWLEDGMENTS

One of the authors (D.M.) was supported by the Swiss National Science Foundation; three of the authors (P.B., K.I.G., and G.K.) were supported in part by AFOSR Grant No. 76-2960.

APPENDIX

Integrals of the form

$$I = \int_0^\infty dx\, x J_0(rx) f(x), \quad r > 0 \tag{A1}$$

with the symmetry

$$f(x) = f(-x) \tag{A2}$$

can be evaluated as follows. Noting $I = \frac{1}{2}(I^{(1)} + I^{(2)})$,

$$I^{(j)} = \int_0^\infty dx\, x H_0^{(j)}(rx) f(x), \quad j = 1, 2 \tag{A3}$$

we can evaluate $I^{(1)}$ by closing the contour counterclockwise at infinity around the first quadrant A_1 and coming down along the positive imaginary axis B_1. We assume here for simplicity that $f(z)$ $(z = x + iy)$, has only simple poles; if there are branch cuts, the corresponding contributions have to be taken into consideration. Then

$$I^{(1)} + A_1 + B_1 = 2\pi i R_1, \tag{A4}$$

where R_1 = residues of $zH_0^{(1)}(rz)f(z)$ at the poles of f in the first quadrant. Similarly,

$$I^{(2)} + A_2 + B_2 = -2\pi i R_4, \tag{A5}$$

where R_4 = residues of $zH_0^{(2)}(rz)f(z)$ at the poles of f in the fourth quadrant. A_2 is the contribution due to the contour at infinity around the fourth quadrant taken clockwise, and B_2 is the contribution coming up along the negative imaginary axis. Obviously, $A_1 = 0$ and $A_2 = 0$ for well-behaved $f(x)$; then

$$2I = I^{(1)} + I^{(2)} = -(B_1 + B_2) + 2\pi i(R_1 - R_4). \tag{A6}$$

R_1 and R_4 are easily evaluated; the essential point is to show that $B_1 + B_2 \equiv 0$ when (A2) is satisfied. This follows upon observing that

$$\begin{aligned} B_1 &= \int_{i\infty}^0 dz\, z H_0^{(1)}(rz) f(z) \\ &= \int_0^\infty dy\, y H_0^{(1)}(rye^{i\pi/2}) f(iy) \\ &= \frac{2}{\pi i} \int_0^\infty dy\, y K_0(ry) f(iy) \end{aligned} \tag{A7}$$

and

$$\begin{aligned} B_2 &= \int_{-i\infty}^0 dz\, z H_0^{(2)}(rz) f(z) \\ &= \int_0^\infty dy\, y H_0^{(2)}(rye^{-i\pi/2}) f(-iy) \\ &= -\frac{2}{\pi i} \int_0^\infty dy\, y K_0(ry) f(-iy). \end{aligned} \tag{A8}$$

The last step in both (A7) and (A8) is based on relations between the Hankel and the modified Bessel functions.[15]

*On leave from Centre de Recherches en Physique des Plasmas, Ecole Polytechnique Fédérale de Lausanne, CH-1007 Lausanne, Switzerland.

[1]K. S. Singwi, M. P. Tosi, R. H. Land, and A. Sjolander, Phys. Rev. 176, 589 (1968); K. S. Singwi, A. Sjolander, M. P. Tosi, and R. H. Land, Solid State Commun. 7, 1503 (1969); Phys. Rev. B 1, 1044 (1970); for an improved version of the STLS approximation scheme, see P. Vashishta and K. S. Singwi, *ibid.* 6, 875 (1973).

[2]J. F. Springer, M. A. Pokrant, and F. A. Stevens, J. Chem. Phys. 58, 4863 (1973); K. Ng, *ibid* 61, 2680 (1974).

[3]K. F. Berggren, Phys. Rev. A 1, 1783 (1970).

[4]H. Totsuji and S. Ichimaru, Prog. Theor. Phys. 50, 753 (1973); 52, 42 (1974); S. Ichimaru, in *Strongly Coupled Plasmas*, edited by G. Kalman (Plenum, New York, 1978), p. 187.

[5]K. I. Golden, G. Kalman, and M. B. Silevitch, Phys. Rev. Lett. 33, 1544 (1974); G. Kalman, T. Datta, and K. I. Golden, Phys. Rev. A 12, 1125 (1975); G. Kalman in *Strongly Coupled Plasmas*, edited by G. Kalman (Plenum, New York, 1978) p. 141; K. I. Golden, *ibid.*, p. 223.

[6]R. Calinon, K. I. Golden, G. Kalman, and D. Merlini, Phys. Rev. A 19, 329 (1979) (preceding paper).

[7]C. Deutsch and M. Lavaud, Phys. Rev. A 9, 2598 (1974).

[8]I. S. Gradshteyn and I. M. Ryzhik, *Tables of Integrals, Series and Products* (Academic, New York, 1965), p. 682.

[9]C. Deutsch, J. Math. Phys. 17, 1404 (1976).

[10]P. Bakshi, G. Kalman, M. B. Silevitch, and K. I. Golden, Bull. Am. Phys. Soc. 21, 1086 (1976); P. Bakshi, in *Strongly Coupled Plasmas*, edited by G. Kalman (Plenum, New York, 1978) p. 533; P. Bakshi, G. Kalman, and M. B. Silevitch (unpublished).

[11]Both the bare and the effective potentials are evidently indeterminate to the extent of an arbitrary constant. As to the bare potential, since $-\ln r \to -\infty$ as $r \to \infty$, it is customary and useful to choose the constant in such a way that $\phi(r) > 0$ within the volume occupied by the system: $\phi(r) = -e^2(\ln r - \ln R)$, where R is of the order of the linear size of the system. As to the screened effective potential, however, since $\Phi(r)$ remains finite as $r \to \infty$, it is useful to choose the constant by requiring $\Phi(r) = 0$ as $r \to \infty$. Unfortunately, this choice leads to $\Phi(r) = -e^2(\ln r - \ln \kappa^{-1})$ for $r \to 0$ and $\Phi(r) \neq \phi(r)$ even in the $r \to 0$ limit. Thus the statement that $\Phi(r) \to \phi(r)$ for $r \to 0$ should be understood with the qualification, "up to a constant." Although the alternative possibility, namely, defining $\phi(r)$ as $\phi(r) = -e^2(\ln r - \ln \kappa^{-1})$, has been put forward, it seems to be unattractive for at least two reasons: (i) since normally $\kappa^{-1} \ll R$, a large $\phi(r) < 0$ domain develops within the system, which gives rise to a non-physical positive contribution to the correlation energy; (ii) since κ is temperature and density dependent, different systems would be characterized by different interaction potentials, and this difference could show up in non-physical temperature- and density-dependent terms in the thermodynamic quantities.

[12]J. P. Hansen, Phys. Rev. A 8, 3096 (1973); H. DeWitt, in *Strongly Coupled Plasmas*, edited by G. Kalman (Plenum, New York, 1978) p. 81.

[13]P. Bakshi, R. Calinon, K. Golden, G. Kalman, and D. Merlini (unpublished).

[14]F. Del Rio and H. E. DeWitt, Phys. Fluids 12, 1404 (1969); C. Deutsch, Y. Furutani, and M. Gombert, Phys. Rev. A 13, 2244 (1976).

[15]M. Abramowitz and I. Stegun, *Handbook of Mathematical Functions* (Dover, New York, 1965), p. 375.